

Stabilization, Selection, and Tracking of Unstable Patterns by Fourier Space Techniques

R. Martin, A. J. Scroggie, G.-L. Oppo, and W.J. Firth

*Department of Physics and Applied Physics, University of Strathclyde, 107 Rottenrow,
Glasgow, G4 0NG, Scotland, United Kingdom*

(Received 8 July 1996)

A new method for the stabilization and manipulation of unstable states of a pattern forming system is presented. The technique is applied to an optical system where unstable homogeneous solutions, rolls, squares, hexagons, and honeycombs are all stabilized and tracked. The control consists of a small spatial modulation to the input pump field, which is derived from the Fourier transform of the output electric field. Once stabilization is achieved, the control vanishes. The method can be used as a numerical tool for pattern forming systems to determine the existence and stability of solutions. [S0031-9007(96)01565-7]

PACS numbers: 42.65.Sf, 47.54.+r

Considerable effort has been made recently to suppress temporal [1–3] and spatiotemporal disorder [4–12] in chaotic regimes. This would allow complex systems to be operated in highly nonlinear regimes while retaining temporal and/or spatial coherence, a desirable feature in fields as diverse as laser physics, plasma physics, and hydrodynamics. A separate, yet related, aim is not only to suppress spatiotemporal chaos, but also to stabilize and manipulate unstable spatial states [4,11,12]. This could have technological applications in, for example, information processing, for which optics is of great interest.

Recently there have been reports of spatiotemporal control in optical models [13,14]. Optical systems display, on fast time scales, phenomena common to many spatially extended systems. One such phenomenon is that of pattern formation, where a spatially extended system may possess a large number of unstable pattern states even in the presence of a stable output. This is associated with the breaking of the rotational and translational symmetry of the system. In this Letter, we present a technique which allows us to select, stabilize, and track such unstable states. This differs from the types of control lately applied to temporal systems which require chaotic dynamics to provide a large number of unstable states. They usually also rely on the ergodicity of the motion to eventually take the system to the desired region of the phase space.

Our method relies upon the fact that a spatially extended system can have a simplified representation in Fourier space. This formed the basis of the control technique used in [10] to suppress 1D spatiotemporal chaotic motion. The features which we will discuss and use in our control are found in the spatial Fourier transform of the electric field and are common to many pattern forming optical systems. Similar properties can also be found in other types of driven dissipative nonlinear systems with rotational invariance [15]. This technique is therefore of general relevance.

It is also important to note that the Fourier transform (or far field) in an optical system is routinely obtainable

in experiments using a single lens. This provides the prospect of the technique being applied in a fully optical manner. It can thus take full advantage of the speed that such systems offer, because all-optical (analog) control is limited only by the response speed of the system.

We consider the mean-field model for a two-level medium in an optical cavity [16,17]. In the good cavity limit, the polarization and population difference variables can be removed by adiabatic elimination. The intracavity electric field is then described by [16,17]

$$\partial_t E = -E \left[(1 + i\theta) + \frac{2C(1 - i\Delta)}{|E|^2 + 1 + \Delta^2} \right] + E_I + i(\partial_{xx} + \partial_{yy})E. \quad (1)$$

Here θ is the cavity detuning, Δ the atomic detuning, $2C$ the medium density expressed as an optical absorptivity, and E_I is the spatially dependent input pump field. Also, the time t has been scaled by the cavity decay time. For simplicity we restrict ourselves to the purely absorptive ($\Delta = 0$) case, the behavior of which is typical of the region $|\Delta| \lesssim 1$ [18]. Then, for a plane-wave pump field E_I , Eq. (1) has stationary, homogeneous solutions E_s given by [17]

$$\frac{E_I}{E_s} = 1 + i\theta + \frac{2C}{|E_s|^2 + 1}. \quad (2)$$

These solutions become unstable for values of C and $I = |E_s|^2$ satisfying

$$\frac{(I + 1)^2}{(I - 1)} < 2C. \quad (3)$$

Close to this “modulational instability” (MI) threshold, the minimum of which is found at $C = 4.0$, perturbations of the form $e^{i\mathbf{K}\cdot\mathbf{r}}$ experience growth if $|\mathbf{K}| \approx K_c \pm \varepsilon$, where ε is small and $K_c = \sqrt{-\theta}$. The condition on \mathbf{K} defines an annulus in Fourier space in which modes grow and destabilize the homogeneous solution. Previous analytical and numerical work has shown that in this system competition between these modes leads eventually

to a steady state consisting of either two (“rolls”) or six (“hexagon”) equally spaced modes. These steady states are, to lowest order, a superposition of a small number of Fourier components. For the purposes of describing our control technique we will label eight wave vectors in Fourier space as in Fig. 1. The absolute orientation of the wave vectors corresponding to these modes is arbitrary, due to the rotational invariance of (1). From this set of wave vectors we can construct all the patterns which we will discuss and stabilize with our control. Rolls are formed by wave vectors $\mathbf{K}_{1,5}$, squares by $\mathbf{K}_{1,3,5,7}$, and hexagons by $\mathbf{K}_{1,2,4,5,6,8}$. In the case of rolls, for example, the field obeys [19]

$$\frac{E}{E_s} - 1 = \frac{1}{2} (|A|e^{i\phi_1} e^{i\mathbf{K}_1 \cdot \mathbf{r}} + |A|e^{i\phi_5} e^{i\mathbf{K}_5 \cdot \mathbf{r}}) + \text{h.o.t.}, \quad (4)$$

where $Ae^{i\phi_i}$ is the complex amplitude associated with the wave vector \mathbf{K}_i , with A real, and h.o.t. represents higher order terms. For the two types of hexagonal patterns, which we denote H^+ and H^- , the field is given by

$$\frac{E}{E_s} - 1 = \frac{1}{2} (|A|e^{i\phi_1} e^{i\mathbf{K}_1 \cdot \mathbf{r}} + |A|e^{i\phi_4} e^{i\mathbf{K}_4 \cdot \mathbf{r}} + |A|e^{i\phi_6} e^{i\mathbf{K}_6 \cdot \mathbf{r}} + \text{c.c.}) + \text{h.o.t.} \quad (5)$$

For $\phi_1 + \phi_4 + \phi_6 = 2n\pi$, these are H^+ hexagons, a hexagonal array of intensity peaks. For $\phi_1 + \phi_4 + \phi_6 = (2n + 1)\pi$, we obtain H^- hexagons, or “honeycombs,” consisting of intensity dips in a bright background. It is important to stress, however, that the amplitudes, relative stability, and even existence of such rolls and hexagons are usually only known in the near threshold region $|A| \ll 1$ [15]. Our control method has no such restriction and can thus be used to establish existence and stability over any range of parameters. For example, for $C = 4.4$, Eq. (3) shows that the homogeneous state is unstable over the range (2.1, 4.7) in I , only the boundaries of which are accurately

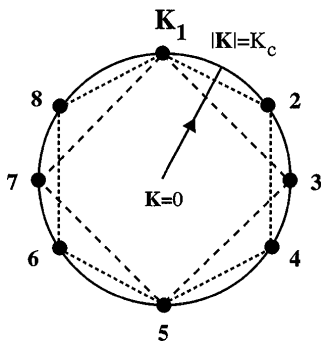


FIG. 1. Schematic diagram of the Fourier modes necessary to form the patterns to which control is applied. The modes lie on the critical circle $|\mathbf{K}| = K_c$. The short dashes indicate the modes which constitute a hexagonal solution, and the long dashes are those necessary for squares.

described by perturbation methods such as amplitude equations [17].

The characteristics of the states we wish to stabilize provide the physical basis for our control technique. As a starting point, to stabilize the homogeneous state above the MI threshold, we must suppress the growth of wave vectors in the instability annulus. First, we take the Fourier transform of the output field and filter it to obtain only the modes contained within the annulus. We then take the inverse Fourier transform of the resulting field, multiply it by a small strength parameter, and subtract it from the input pump field. Thus, the pump field acquires a spatial modulation which is determined only by the modes found in the instability annulus in Fourier space. The pump field can then be written as

$$E_I(x, y) = E_{I0}(1 + F), \quad F = -s_1 f_1(x, y), \quad s_1 > 0, \quad (6)$$

where E_{I0} is the magnitude of the plane-wave pump and s_1 the feedback strength. In this way, we provide negative feedback only for the modes which lie in the annulus. The function $f_1(x, y)$ can be described by

$$f_1(x, y) = \mathcal{F}^{-1} \mathcal{U} \mathcal{F} E, \quad (7)$$

where \mathcal{F} denotes the operation of Fourier transformation of the electric field E , \mathcal{U} describes the filtering operation in Fourier space, and \mathcal{F}^{-1} is the inverse Fourier transformation.

The results which we will present were obtained numerically by integrating Eq. (1), using a split step spectral method. The integrations were performed mainly on a 64×64 grid with a box size of $16\pi/K_c$. Critical cases were also checked on a 128×128 grid. The control was applied in a continuous, stepwise fashion with no delay, being updated every 0.1 units of time with a time step of 0.02 units. This technique is extremely powerful and has allowed us to stabilize the homogeneous state for values of C up to 5.28, which is $>30\%$ above the minimum MI threshold, and we anticipate that it will continue to work for even larger values of C . When the homogeneous state is stabilized, the pump modulation vanishes since the Fourier transform of the field contains no excited wave vectors in the annulus.

In order to control pattern states, we now modify \mathcal{U} in Eq. (7). To stabilize rolls, for example, we remove two diametrically opposite modes ($\mathbf{K}_{1,5}$) of magnitude K_c from the feedback. This allows the formation of rolls by suppressing the growth of all except the desired modes. Again, the feedback vanishes as the rolls stabilize, ensuring that these rolls are indeed a solution of Eq. (1). Because of the rotational degeneracy, we are free to choose the orientation of the stabilized rolls.

The stabilization of patterns of more than two wave vectors requires an extra degree of control. If we now

try to stabilize squares (four wave vectors) by removing the wave vectors $\mathbf{K}_{1,3,5,7}$ from the feedback, we end with the stabilization of rolls in one of the two possible orientations, the roll pattern being more stable than squares. We must ensure the presence of all four wave vectors, and this is done by calculating the control b_i on mode i according to

$$\begin{aligned} b_1 &\propto -a_1 + a_7, & b_5 &\propto -a_5 + a_3, \\ b_3 &\propto -a_3 + a_1, & b_7 &\propto -a_7 + a_5, \end{aligned} \quad (8)$$

where a_i is the amplitude of the wave vector \mathbf{K}_i . This could be achieved experimentally by filtering the Fourier field to obtain the amplitudes a_i and passing the field through an interferometer with a field rotating element in one arm to obtain the amplitudes b_i . We then take the inverse Fourier transform to construct $f_2(x, y)$ which is fed back as *positive* feedback to the pump. The feedback modulation in (6) now becomes

$$F = -s_1 f_1(x, y) + s_2 f_2(x, y), \quad (9)$$

where $s_2 > 0$ and is the strength of the positive feedback.

As well as suppressing unwanted modes, the control (9) distributes the energy among all four wave vectors necessary for the formation of squares via a simple rotation in the Fourier space. The desired pattern is thus stabilized with a feedback control which again disappears when stabilization is achieved. This is a particularly interesting result, since squares were not even known to exist in this system and have never been observed in simulations of Eq. (1). It is important to note that the width of the filter in Fourier space must be chosen such that the spatial harmonics of the desired pattern are not included in the feedback. These modes form a part of the exact solution to (1) and therefore must not be suppressed.

A straightforward extension of (8) also allows the stabilization of hexagonal patterns. As discussed previously, there are two classes of hexagons, distinguished by the sum of the phases of the complex amplitudes being an even (H^+) or odd (H^-) multiple of π . This control stabilizes a hexagonal pattern of either kind, without being able to distinguish between them. It may be necessary for some applications, however, to be able to select between the different types of hexagons. We have found that, by replacing (8) with

$$\begin{aligned} b_1 &\propto -a_1 - a_8, & b_5 &\propto -a_5 - a_4, \\ b_2 &\propto -ia_2 - a_1, & b_6 &\propto -ia_6 + a_5, \\ b_4 &\propto -a_4 - ia_2, & b_8 &\propto -a_8 + ia_6, \end{aligned} \quad (10)$$

we can stabilize the solution with $\phi_1 = \phi_4 = \pi/2$ and $\phi_6 = -\pi$. This is one among a two-dimensional manifold of possibilities, but different choices for $\phi_{1,4,6}$ simply correspond to translating the hexagonal pattern. Instead, to stabilize a H^- hexagon solution with $\phi_1 = \phi_4 = 0$

and $\phi_6 = \pi$, Eq. (10) becomes

$$\begin{aligned} b_1 &\propto -a_1 + a_8, & b_5 &\propto -a_5 + a_4, \\ b_2 &\propto -a_2 - a_1, & b_6 &\propto -a_6 - a_5, \\ b_4 &\propto -a_4 - a_2, & b_8 &\propto -a_8 - a_6. \end{aligned} \quad (11)$$

Our simulations reveal that these schemes are able to distinguish between the two types of hexagonal patterns and stabilize the desired solutions. Experimentally, the implementation of the control for squares and hexagons is the same. However, to differentiate between the two types of hexagons, appropriate phase plates must be added to the Fourier components (beams) in the interferometer.

Figure 2 shows the stable and unstable solutions of the different pattern states which were stabilized and tracked using the control technique. These solution branches are obtained for regions of parameter space far from the MI threshold. In these regions a perturbative description breaks down since the amplitudes of the solutions are no longer guaranteed to be small [17]. Our method, however, provides a numerical tool for mapping out solution branches, where even approximate analytic descriptions fail. It is applicable not only to optical systems but also to simulations of any system displaying this type of pattern formation. Figure 3 shows a dynamical sequence of pattern selection and stabilization. The sequence starts with the formation of rolls, the stable pattern for the given parameters. The control was applied since this allowed faster convergence to the steady state. Then H^+ hexagons, H^- hexagons, squares, and, finally, the

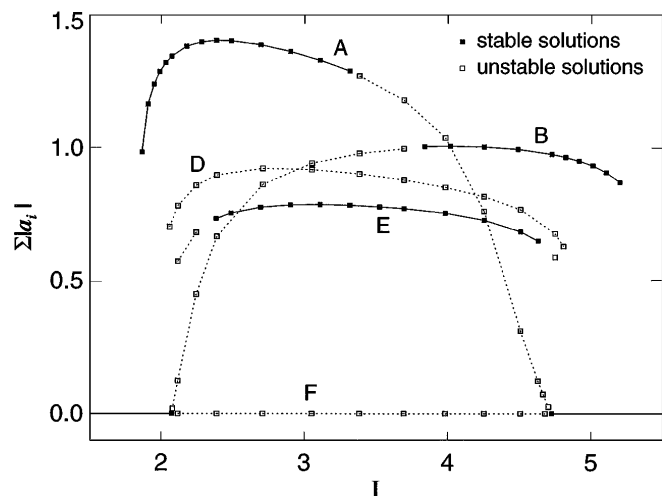


FIG. 2. Plot of stable and unstable solutions over the range $I = (1.5, 5.5)$, with $C = 4.4$ and $\theta = -1.0$. **A** denotes H^+ hexagons, **B** denotes H^- hexagons, **D** denotes squares, **E** denotes rolls, and **F** denotes the homogeneous solution. Each marked point corresponds to a numerical simulation. The stable solutions, joined with solid lines, were obtained without using control. The controlled unstable solutions are joined by broken lines, and the continuity of the curves indicates that these points are indeed solutions of (1). The points were obtained by summing $|a_i|$ of the constituent wave vectors of the patterns.

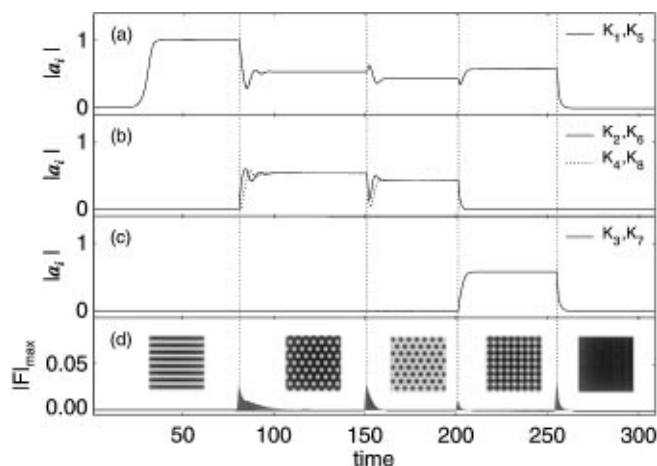


FIG. 3. Dynamical sequence of control and pattern selection for $C = 4.4$, $\theta = -1.0$, and $I = 3.5$. (a) The amplitude (in arbitrary units) of the pair of wave vectors which are selected in all of the stabilized patterns, (b) the other two pairs which are excited in hexagonal patterns, and (c) the pair excited only in squares. (d) The maximum amplitude of the feedback in the same units, along with the patterns stabilized in each region of the figure. For each pattern $s_1 = 0.05$, for hexagons and honeycombs $s_2 = 0.025$, and for squares $s_2 = 0.0125$.

homogeneous solution are all stabilized with appropriate feedback control. As can be seen in Fig. 3(d), the feedback vanishes once control is achieved. Figures 3(a)–3(c) display the amplitudes of the excited wave vectors of the patterns.

In order to establish the robustness of the control technique, we have also simulated Eq. (1) with an additive Gaussian noise term. We were able to achieve control for noise strengths up to 10% of the amplitude of the stable patterns. This, combined with the fact that the Fourier space information is easily obtained optically, suggests that the method can be implemented experimentally. From the point of view of experiments, there are three main ingredients to the technique: Fourier filtering, field rotation, and phase control when superposing fields. All these operations, separately performed to interferometric precision, can be realistically implemented and combined in optical experiments. In fields other than optics, the Fourier transform cannot be obtained directly. However, in systems which evolve slowly, techniques where the feedback is evaluated by computer can be applied [7].

We have presented a control method which allows the selection, stabilization, and tracking of unstable patterns. Depending on the target pattern and the coexisting stable and unstable states, a control technique can be constructed consisting of both positive and negative feedback elements to the spatially extended input pump field. The positive feedback element encourages the desired Fourier modes to grow, and the negative feedback suppresses un-

wanted modes. The method has been applied successfully to a model of a nonlinear optical cavity and has allowed the determination of unstable pattern solution branches of the system, which, so far, have been unobtainable both analytically and numerically. The technique is powerful, flexible, and robust against noise and allows the stabilization of any unstable pattern state which has a simple Fourier space description, from both pattern and low amplitude noise initial conditions. These are fundamental requirements for any potential application of such a control technique. We expect that the method could be realistically applied to optical experiments, and, as a first test of its generality, the technique has also been applied successfully in a laser system [20].

We acknowledge G. K. Harkness for useful discussions and the EPSRC for financial support (Grant J/30998). R. M. acknowledges an EPSRC studentship.

-
- [1] E. Ott, C. Grebogi, and J. A. Yorke, *Phys. Rev. Lett.* **64**, 1196 (1990).
 - [2] E. R. Hunt, *Phys. Rev. Lett.* **67**, 1953 (1991).
 - [3] K. Pyragas, *Phys. Lett. A* **170**, 421 (1992).
 - [4] J. A. Sepulchre and A. Babloyantz, *Phys. Rev. E* **48**, 945 (1993).
 - [5] H. Gang and H. Kaifen, *Phys. Rev. Lett.* **71**, 3794 (1993).
 - [6] D. Auerbach, *Phys. Rev. Lett.* **72**, 1184 (1994).
 - [7] F. Qin, E. E. Wolf, and H.-C. Chang, *Phys. Rev. Lett.* **72**, 1459 (1994).
 - [8] I. Aranson, H. Levine, and L. Tsimring, *Phys. Rev. Lett.* **72**, 2561 (1994).
 - [9] G. A. Johnson, M. Löcher, and E. R. Hunt, *Phys. Rev. E* **51**, R1625 (1995).
 - [10] C. Lourenço, M. Hougardy, and A. Babloyantz, *Phys. Rev. E* **52**, 1528 (1995).
 - [11] V. Petrov, S. Metens, P. Borckmans, G. Dewel, and K. Showalter, *Phys. Rev. Lett.* **75**, 2895 (1995).
 - [12] A. Hagberg, E. Meron, I. Rubinstein, and B. Zaltzman, *Phys. Rev. Lett.* **76**, 427 (1996).
 - [13] W. Lu, D. Yu, and R. G. Harrison, *Phys. Rev. Lett.* **76**, 3316 (1996).
 - [14] R. Martin, A. J. Kent, G. D'Alessandro, and G. L. Oppo, *Opt. Commun.* **127**, 161 (1996).
 - [15] M. C. Cross and P. C. Hohenberg, *Rev. Mod. Phys.* **65**, 851 (1993).
 - [16] L. A. Lugiato and C. Oldano, *Phys. Rev. A* **37**, 3896 (1988).
 - [17] W. J. Firth and A. J. Scroggie, *Europhys. Lett.* **26**, 521 (1994).
 - [18] A. J. Scroggie, Ph.D. Thesis, University of Strathclyde, 1995 (unpublished).
 - [19] S. Ciliberto, P. Coullet, J. Lega, E. Pampaloni, and C. Perez-Garcia, *Phys. Rev. Lett.* **65**, 2370 (1990).
 - [20] G. K. Harkness (private communication).